

Features of $\text{Ca}_{1-x}\text{Y}_x\text{F}_{2+x}$ solid solution heat capacity behavior: diffuse phase transition

Alexander A. Alexandrov^{1,2,a}, Anna D. Rezaeva^{1,b}, Vasilii A. Konyushkin^{1,c},
Andrey N. Nakladov^{1,d}, Sergey V. Kuznetsov^{1,e}, Pavel P. Fedorov^{1,f}

¹Prokhorov General Physics Institute of the Russian Academy of Sciences, Moscow Russia

²Kurnakov Institute of General and Inorganic Chemistry of the Russian Academy of Sciences, Moscow, Russia

^aalexandrov1996@yandex.ru, ^b1032192969@rudn.ru, ^cvasil@lst.gpi.ru,

^dandy-nak@yandex.ru, ^ekouznetsovsv@gmail.com, ^fppfedorov@yandex.ru

Corresponding author: Pavel P. Fedorov, ppfedorov@yandex.ru

ABSTRACT A series of single crystals of a $\text{Ca}_{1-x}\text{Y}_x\text{F}_{2+x}$ solid solution with a fluorite structure containing 1–19 mol.% YF_3 ($x = 0.01–0.19$) has been grown. Thermal analyzer STA 449 F3 Jupiter in DSC mode recorded the temperature dependences of the heat capacity $C_p(T)$ in the temperature range from the room temperature to 1300 °C. A diffuse phase transition in the solid state for concentrations $x = 0.01–0.03$ is fixed as an anomaly on the $C_p(T)$ curves with a maximum at 1150 ± 50 °C. With an increase in the content of YF_3 ($x = 0.05–0.19$), a very wide structured peak is recorded in the range of 650–1100 °C. The heat capacity anomaly is associated with the reversible rearrangement of defect nanoclusters, which affects the change in the anion sublattice.

KEYWORDS $\text{CaF}_2\text{--YF}_3$ phase diagram, inorganic fluorides, fluorite, diffuse phase transition, solid solution, heterovalent isomorphism, defect clusters.

ACKNOWLEDGEMENTS Authors express their sincere gratitude to E. V. Chernova for her most kind assistance in the preparation of the present manuscript. The study was funded by grant of Russian Science Foundation No. 22-13-00167, <https://rscf.ru/project/22-13-00167>.

FOR CITATION Alexandrov A.A., Rezaeva A.D., Konyushkin V.A., Nakladov A.N., Kuznetsov S.V., Fedorov P.P. Features of $\text{Ca}_{1-x}\text{Y}_x\text{F}_{2+x}$ solid solution heat capacity behavior: diffuse phase transition. *Nanosystems: Phys. Chem. Math.*, 2023, **14** (2), 279–285.

1. Introduction

Compounds with the fluorite-type crystal structure ($Fm\bar{3}m$ space symmetry group) include MF_2 difluorides ($M = \text{Ca}, \text{Sr}, \text{Ba}, \text{Cd}$, higher temperature polymorph of PbF_2) as well as SrCl_2 , UO_2 and CeO_2 . At $T \sim (0.7–0.8) \cdot T_{\text{melting}}$, all these substances exhibit the very specific anomaly in their physical properties that has been named as diffuse phase transition [1–14]. The term “Faraday transition” has been also suggested for such a phenomenon because it has been described for PbF_2 by Michael Faraday in 1834 [9]. Experimental data for the heat capacity, thermal expansion, ionic conductivity, elastic constants and other physical properties, including neutron scattering and Brillouin scattering patterns of the aforementioned substances, confirm the said anomaly. The mechanism of the diffuse phase transition is well-known, and it is described in terms of the interaction between point anti-Frenkel anionic defects [5, 10] and soft phonon modes [12]. The concentration of the latter defects increases with the temperature increase, resulting in cooperative interaction between the individual defects and disordering of the anionic sublattice (“sublattice melting”). The high-temperature form of fluorite MX_2 compounds is characterized by formation of complex short-living defect clusters containing an excess of interstitial anions, anionic vacancies and relaxed lattice anions [7, 11]. The diffuse phase transition is accompanied by an increase in the anionic conductivity and transition of MF_2 to the superionic state [6].

Thoroughly conducted thermochemical experiments [1, 4] and simulations [5, 12–14] indicate that, for all diffuse phase transitions, one have only observed an anomaly in the heat capacities as relatively wide (half-width about 200 K) maxima in the curves describing the temperature dependences of the $C_p(T)$ values, while there were no thermal analysis data confirming the existence of the first- or second order phase transitions, or effects indicating non-zero enthalpies of the said first order phase transitions [10]. Thorough measurements of the thermal expansion coefficients for the specimens in the fluorite-type compounds [8] also have revealed the similar anomalies for the temperature dependences of the said coefficients.

The above said CaF_2 heat capacity maximum [1] indicates only that the thermodynamic stability of the corresponding system goes through its minimum. This situation can be characterized as the “flag of catastrophe” from the catastrophe theory [15] point of view, and the said diffuse phase transition is not a real first or second order phase transition from the thermodynamic point of view: the same phase of the same space symmetry group just maintains its existence.

In binary systems involving components undergoing a diffuse phase transition, there are anomalies on the curve of the maximum concentration of solid solution (solvus). In many systems, solvus curves have an abnormal S-type shape. Such curve shape is caused by the factor that the higher temperature disordered form of fluorites is more prone to the heterovalent isomorphism than the lower temperature forms [16]. For example, a clearly expressed S-type solvus curve exists in the $\text{CaF}_2\text{-LaF}_3$ [17] and $\text{SrF}_2\text{-LaF}_3$ [18] systems. A very complex profile of the solidus curve for the CaF_2 -based solid solution has been observed in the NaF-CaF_2 system [19].

The division of the fluorite-type region of solid solutions in binary systems into high-temperature and low-temperature regions suggests that the temperature band of the diffuse phase transition should go to the low-temperature region when the matrix is doped with an isomorphous component. This assumption, put forward in [16], was confirmed both in thermodynamic modeling and in separate measurements of some physical properties, including ionic conductivity [10, 20–22]. However, this hypothesis has not been systematically tested before.

The purpose of this work is to test the behavior of the diffuse phase transition in calcium fluoride when the CaF_2 matrix is doped with yttrium fluoride. The $\text{CaF}_2\text{-YF}_3$ system is a classical system, which is used as an example for illustration of the mechanism of heterovalent isomorphism, in particular, the formation of the mineral yttrifluorite [23, 24]. This is a model system describing the behavior of other rare-earth fluorides of the yttrium subgroup. The phase diagram of $\text{CaF}_2\text{-YF}_3$ systems has been carefully studied [25–29], see Fig. 1 [30, 31]. A fluorite solid solution $\text{Ca}_{1-x}\text{Y}_x\text{F}_{2+x}$ (phase F), a series of ordered low-temperature fluorite-like phases, and a high-temperature non-stoichiometric phase with a tysonite structure (phase T) are formed in the system. The maximum on the melting curve of the $\text{Ca}_{1-x}\text{Y}_x\text{F}_{2+x}$ fluorite solid solution at $x = 0.11$ (11 mol.% YF_3) is the source of functional optical single-crystal materials [32, 33].

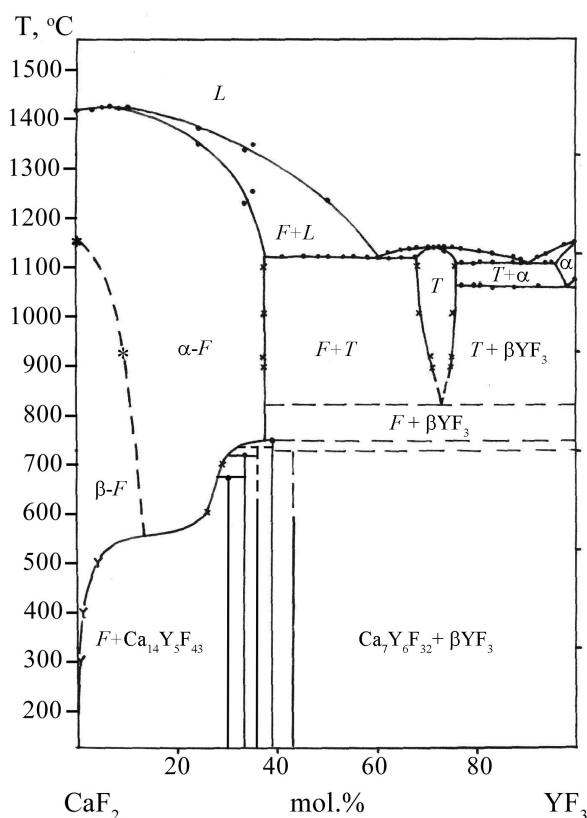


FIG. 1. Phase diagrams of the $\text{CaF}_2\text{-YF}_3$ systems [30,31]

The dotted line dividing the $\text{Ca}_{1-x}\text{Y}_x\text{F}_{2+x}$ solid solution field (phase F) into two parts (α and β) in Fig. 1 reflects the ideas concerning to the behavior of the diffuse phase transition with the change of concentration that took place before our work began.

2. Experimental

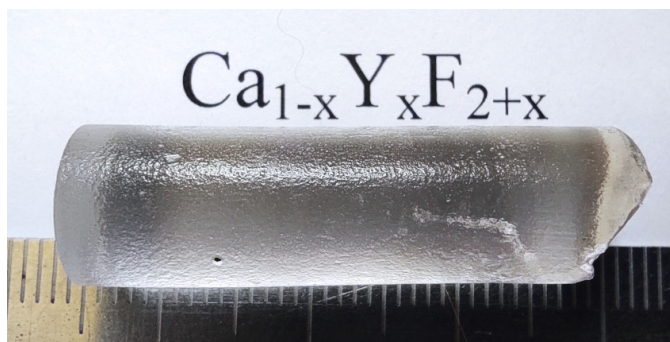
CaF_2 (optical crystals shards, State Optical Institute, St.-Petersburg) and YF_3 (99.99 wt%, LANHIT, Moscow) were used as the starting reagents.

$\text{Ca}_{1-x}\text{Y}_x\text{F}_{2+x}$ single crystals, where $x = 0, 0.01, 0.03, 0.05, 0.07, 0.10, 0.12, 0.15$ (nominal compositions), 10 mm in diameter, 45 mm long, were grown by the Bridgman-Stockbarger technique (Fig. 2). A portion of the initial mixture was loaded into a seven-channel graphite crucible and placed in a growth setup. The growth chamber was preliminarily

TABLE 1. Characteristics of the studied samples of the $Ca_{1-x}Y_xF_{2+x}$ single crystals

Number	Nominal composition, mol% YF_3	Lattice parameter a , Å	EDX data, mol% YF_3
1	1.0	5.4664	1.2
2	3.0	5.4686	2.9
3	5.0	5.4732	5.6
4	7.0	5.4786	7.6
5	10.0	5.4834	12.4
6	12.0	5.4893	14.0
7	15.0	5.4976	19.2

evacuated to 10^{-2} Torr. The crucible was heated to the charge melting temperature of 1440°C . The melt was fluorinated by CF_4 and then crucible pulled into the cold zone at a rate of 5 mm/h. After growth, the crystals were removed from the crucible and purified of graphite by mechanical treatment and ethanol. A plate with a diameter of 10 mm and a thickness of 1 mm was cut from the crystal, which was then ground in a jasper mortar. The grown $Ca_{1-x}Y_xF_{2+x}$ crystals did not have a characteristic optical heterogeneity – a cellular substructure [34].

FIG. 2. $Ca_{1-x}Y_xF_{2+x}$ single crystal (sample number 6, $x = 0.14$)

X-ray phase analysis was performed on a Bruker D8 Advance diffractometer (Germany) with $CuK\alpha$ radiation in the angle range from 15 to $80^\circ 2\theta$ with a step of 0.02° and a signal accumulation time of 0.4 s per point. Elemental analysis was performed on a Carl Zeiss NVision 40 microscope with an Oxford Instruments X-MAX 80 mm^2 attachment on powder samples with the accumulation of several spectra for statistical significance.

The samples were measured on a STA 449 F3 Jupiter synchronous thermal analysis instrument using a Type S DSC sensor and platinum-rhodium crucibles. The heating rate was $20^\circ\text{C}/\text{min}$. The weighed portions of the powders (20 – 50 mg) were placed in Pt–Rh crucibles and covered with a lid. The reference crucible remained empty in all dimensions. The argon flow into the furnace chamber was $70\text{ ml}/\text{min}$. The maximum temperature was 1330°C . A sapphire standard 5.2 mm in diameter and 0.25 mm thick was used as a reference.

The heat capacity was calculated using formula (1):

$$C_p = \frac{m_{\text{Standart}}}{m_{\text{Sample}}} \cdot \frac{DSC_{\text{Sample}} - DSC_{\text{Baseline}}}{DSC_{\text{Standart}} - DSC_{\text{Baseline}}} \cdot C_{p,\text{Standart}}, \quad (1)$$

by software Netzsch Proteus Thermal Analysis with using ASTM E 1257, ISO 11357-4, DIN 51007 standards.

3. Results and discussion

The lattice parameters and compositions evaluated by EDX for samples are summarized in Table 1. The temperature dependences of the specific heat capacity are shown in Fig. 3.

When evaluating the measurement results (Fig. 3), it should be noted that the absolute values of the heat capacity cannot be trusted, except for the low-temperature (up to 800°C) range for pure CaF_2 (Fig. 3a). In all other cases, the measurements obtained during the second and third heatings differ sharply in magnitude. The reasons for this are not entirely clear. They can be associated both with a change in the degree of compactness of the powder (sintering) and with the partial preservation of the high-temperature defective structure of the sample after heat treatment. However, some characteristic features of the observed anomaly on the $C_p(T)$ curves remain, which will be the subject of analysis.

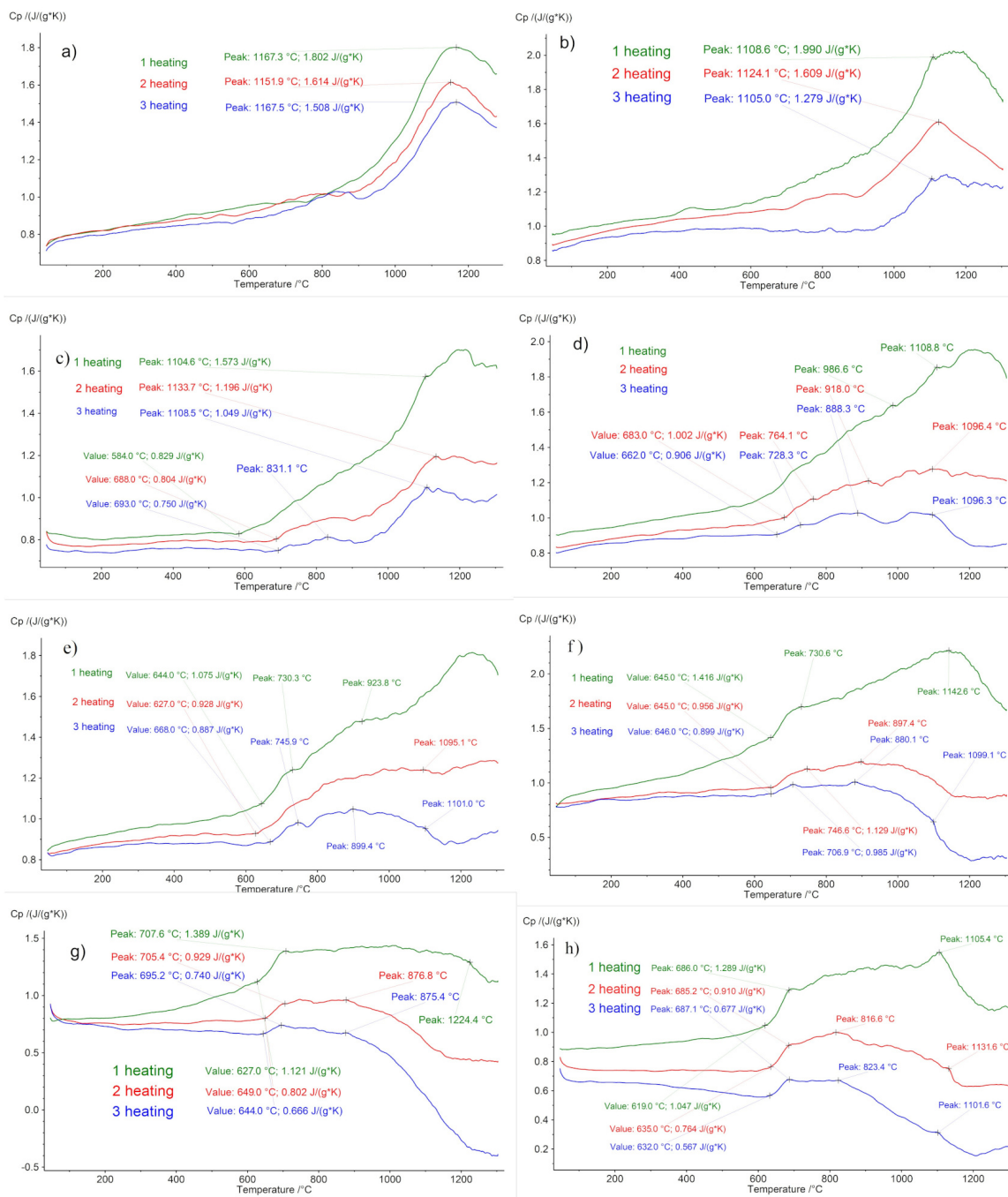


FIG. 3. Temperature dependences of the specific heat capacity. Nominal composition: a – CaF_2 , b – sample number 1, c – sample number 2, d – sample number 3, e – sample number 4, f – sample number 5, g – sample number 6, h – sample number 7

For pure calcium fluoride (Fig. 3a), the maximum temperature of the $C_p(T)$ curve corresponds to the results of Naylor [1]. At a low impurity content (~ 1 mol % YF_3), the character of the dependence changes slightly, although the specific heat capacity peak is somewhat broadened (Fig. 3b). In this case, the beginning of the effects cannot be distinguished.

With an increase in the content of yttrium fluoride, the nature of the temperature dependencies of the specific heat capacity changes significantly. A low temperature component appears, a pronounced onset of the effects is formed, the specific heat capacity anomaly is structured, and starting from 10 mol.% YF_3 , three extrema can be clearly distinguished on it (Fig. 3(f–h)). With a change in the concentration of yttrium fluoride, the temperatures of these effects change slightly, staying within 600–1150 °C (Fig. 4). This behavior differs sharply from the initial expectation of a monotonic decrease in the maximum at the specific heat capacity anomaly with increasing temperature.

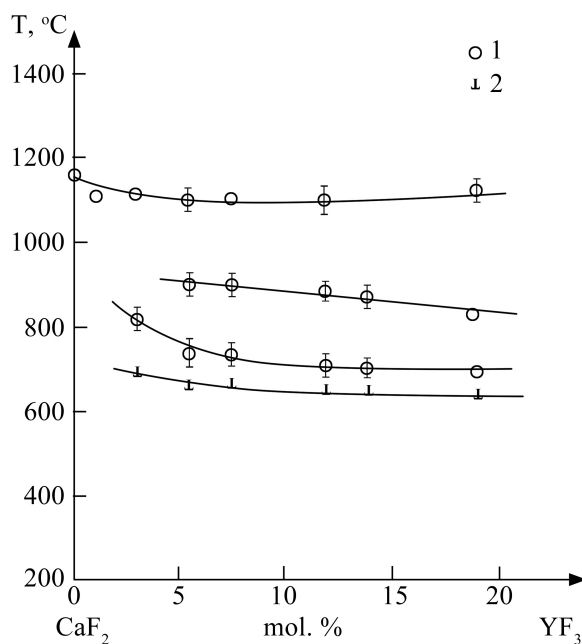


FIG. 4. Temperatures of heat capacity anomalies in $\text{Ca}_{1-x}\text{Y}_x\text{F}_{2+x}$ single crystals. 1 – peak position, 2 – onset. Lines are guides to the eyes

Apparently, the observed effects can be associated with the rearrangement of defect clusters. Since these effects are at least partially reversible upon heating-cooling, it can be concluded that the rearrangement is mainly associated with changes in the anionic sublattice.

Usually, when discussing the cluster structure of defects in heterovalent solid solutions, rearrangements with increasing concentration are considered, leaving aside the effect of temperature [35]. One of few exceptions is the work of Osiko [36].

Structural investigations of $\text{Ca}_{1-x}\text{Y}_x\text{F}_{2+x}$ solid solution and analogues systems were objects of numerous works. The complexity of the cluster structures has been revealed by X-ray diffraction, spin resonance, spectroscopic, extended X-ray-absorption fine structure (EXAFS), MNR ^{19}F and computer simulation techniques [37–44]. Dipoles $\text{Y}^{3+}\text{--F}_{int}^-$, formed at a low content of YF_3 in the solid solution, rapidly undergo further association with increasing concentration. Dimers $(\text{Y}^{3+}\text{--F}_{int}^-)_2$ [36] transform into so-called 2:2:2 clusters due to the relaxation of the anionic sublattice [39]. To describe the structure formed at a high concentration of yttrium fluoride, very exotic models were initially proposed [38], which were replaced by the Y_6F_{37} cubooctahedral cluster [41, 45–47]. The size of such clusters with their defective periphery is about 1.5 nm. It is these clusters that form the basis of ordered fluorite-like phases in the $\text{CaF}_2\text{--YF}_3$ system.

The presence of a dominant type of clusters does not exclude the existence of a wide range of clusters in crystals. The set of coordination polyhedra of rare-earth elements in solid solutions leads to a broadening of the luminescence spectra with transition to the disordered structure, see, for example, [48].

Clustering causes an increase in electrical conductivity with concentration [49, 50]. The composition containing ~ 3 mol.% YF_3 approximately corresponds to the so-called percolation threshold, i.e. association of clusters (their defective periphery) into a single network in the bulk of the crystal [49].

As for high-temperature studies, the study of Catlow e.a [42] of a similar system $\text{Ca}_{0.9}\text{Er}_{0.1}\text{F}_{2.1}$ by the EXAFS method in the range of 298–1070 K did not record noticeable changes. In the context of this work, the investigation by Hoffmann et al. [43] devoted to the study of the crystal structure of $\text{Ca}_{0.94}\text{Y}_{0.06}\text{F}_{2.06}$ at different temperatures up to 1400 K is of particular importance. Hoffmann et al., using the neutron diffraction technique, recorded the destruction of cubooctahedral Y_6F_{37} cluster starting from ~ 630 °C and their complete disappearance at ~ 900 °C.

4. Conclusions

In this paper, new and unexpected data were obtained concerning the manifestations of a diffuse phase transition in a heterovalent $\text{Ca}_{1-x}\text{Y}_x\text{F}_{2+x}$ solid solution with a fluorite structure. The obtained data indicate the rearrangement of defect nanoclusters not only with concentration, but also with temperature. The relevant instructions open up a new way to control the functional properties of materials based on the corresponding solid solutions. Of paramount interest are both studies of this phenomenon by a complex of structural and physicochemical methods, and a detailed study of similar systems. An interesting and promising problem is the possible implementation of diffuse phase transitions in high-temperature cubic polymorphs of ZrO_2 and HfO_2 and solid solutions based on them.

References

- [1] Naylor B.F. Heat contents at high temperatures of magnesium and calcium fluorides. *J. Amer. Chem. Soc.*, 1945, **67**, P. 150–152.
- [2] Bredig M.A. The order-disorder (I) transition in UO_2 and other solids of the fluorite type of structure. *Colloq. Inter. CNRS*, 1972, **205**, P. 183–197.
- [3] Catlow C.R.A., Comings J.D., Germano F.A., Harley R.T. Hayes W. Brillouin scattering and theoretical studies of high-temperature disorder in fluorite crystals. *J. Phys. C: Solid State Phys.*, 1978, **11**, P. 3197–3212.
- [4] Schröter W., Nölting J. Specific heats of crystals with the fluorite structure. *J. Phys. Coll. (Paris)*, 1980, **41**, P. 6–20.
- [5] Oberschmidt J. Simple thermodynamic model for the specific-heat anomaly and several other properties of crystals with the fluorite structure. *Phys. Rev. B*, 1981, **23**, P. 5038–5047.
- [6] Chadwick A.V. High-temperature transport in fluorites. *Solid State Ionics*, 1983, **8**, P. 209–220.
- [7] Hutchings M.T., Clausen K., Dickens M.H., Hayes W., Kjems J.K., Schnabel P.G., Smith C. Investigation of thermally induced anion disorder in fluorites using neutron scattering techniques. *J. Phys. C*, 1984, **17**, P. 3903–3940.
- [8] Roberts R.B., White G.K. Thermal expansion of fluorites at high temperatures. *J. Phys. C*, 1986, **19**, P. 7167–7172.
- [9] Hull S. Superionics: crystal structures and conduction processes. *Rep. Prog. Phys.* 2004, **67**, P. 1233–1314.
- [10] Vlieg E., den Hartog H.W. The superionic phase transition of fluorite-type crystals. *J. Phys. Chem. Solids*, 1986, **47**(5), P. 521–528.
- [11] Allnatt A.R., Chadwick A.V., Jacobs P.W.M. A model for the onset of fast-ion conduction in fluorites. *Proc. R. Soc. London A*, 1987, **410**, P. 385–408.
- [12] Schmalzl K., Strauch D., Schober H. Lattice-dynamical and ground-state properties of CaF_2 studied by inelastic neutron scattering and density-functional methods. *Phys. Rev. B*, 2003, **68**, P. 144301–144313.
- [13] Eapen J., Annamareddy A. Entropic crossovers in superionic fluorites from specific heat. *Ionics*, 2017, **23**, P. 1043–1047.
- [14] Fossati P.C.M., Chartier A., Boulle A. Structural aspects of the superionic transition in AX_2 compounds with the fluorite structure. *Frontiers in Chemistry*, 2021, **9**, # 723507 (19 pp.)
- [15] Gilmore R. *Catastrophe Theory for Scientists and Engineers*. New York, Dover, 1993.
- [16] Fedorov P.P., Sobolev B.P. Phase diagrams of the CaF_2 –(Y,Ln) F_3 systems. II. A discussion. *J. Less-Common Metals*, 1979, **63**, P. 31–44.
- [17] Svantner M., Mariani E., Fedorov P.P., Sobolev B.P. Solid solution with fluorite structure in the CaF_2 – LaF_3 system. *Kristall und Technik-Crystal Research and Technology*, 1979, **14**(3), P. 365–369.
- [18] Fedorov P.P., Alexandrov A.A., Voronov V.V., Mayakova M.N., Baranchikov A.E., Ivanov V.K. Low-temperature phase formation in the SrF_2 – LaF_3 system. *J. Amer. Ceram. Soc.*, 2021, **104**(6), P. 2836–2848.
- [19] Fedorov P.P., Maykova M.N., Kuznetsov S.V., Maslov V.A., Sorokin N.I., Baranchikov A.E., Ivanov V.K., Pynenkov A.A., Uslamina M.A., Nishchev K.N. Phase Diagram of the NaF – CaF_2 System and the Electrical Conductivity of a CaF_2 -Based Solid Solution. *Russ. J. Inorg. Chem.*, 2016, **61**(11), P. 1472–1478.
- [20] Catlow C.R.A., Comins J.D., Germano F.A., Harley R.T. Hayes W., Owen I.B. Studies of effects of trivalent impurity ions on the transition to the superionic state of fluorites. *J. Phys. C: Solid State Phys.*, 1981, **14**, P. 329–335.
- [21] Andersen N.H., Clausen K., Kjems J.K. Heavily doped $\text{M}_{1-x}\text{U}_x\text{F}_{2+2x}$ fluorites studied by quasielastic neutron scattering ($\text{M} = \text{Ba}$) and specific heat measurements ($\text{M} = \text{Pb}$). *Solid State Ionics*, 1983, **9–10**, P. 543–548.
- [22] Ouwerkerk M., Kelder E.M., Schoonman J. Conductivity and specific heat of fluorites $\text{M}_{1-x}\text{U}_x\text{F}_{2+2x}$ ($\text{M} = \text{Ca}, \text{Sr}, \text{Ba}$ and Pb). *Solid State Ionics*, 1983, **9–10**, P. 531–536.
- [23] Bokii G.B. *Kristalokhimiya (Crystal Chemistry)*. M.: Nauka, 1971. (in Russian)
- [24] Filatov S.K., Krivovichev S.V., Bubnova R.S. *Obschaya kristalokhimiya (General Crystal Chemistry)*. S.-Peterburg: Izd. SPbGU, 2018. (in Russian)
- [25] Seiranian K.B., Fedorov P.P., Garashina L.S., Molev G.V., Karelin V.V., Sobolev B.P. Phase diagram of the system CaF_2 – YF_3 . *J. Crystal Growth*, 1974, **26**(1), P. 61–64.
- [26] Fedorov P.P., Izotova O.E., Alexandrov V.B., Sobolev B.P. New phases with fluorite-derived structure in CaF_2 –(Y, Ln) F_3 systems. *J. Solid State Chem.*, 1974, **9**(4), P. 368–374.
- [27] Gettmann W., Greis O. Über fluorit- und tysonitverwandte ordnungsphasen im system CaF_2 – YF_3 . *J. Solid State Chem.*, 1978, **26**(3), P. 255–263.
- [28] Greis O., Haschke J.M. *Rare Earth Fluorides. Handbook on the Physics and Chemistry of Rare Earth*. Ed. K.A. Gscheidner & L. Eyring. Amsterdam, New York, Oxford. 1982, **5**, Ch. 45, P. 387–460.
- [29] Sobolev B.P., Fedorov P.P. Phase diagrams of the CaF_2 –(Y,Ln) F_3 systems. I. Experimental. *J. Less-Common Metals*, 1978, **60**, P. 33–46.
- [30] Fedorov P.P. Third law of thermodynamics as applied to phase diagrams. *Rus. J. Inorg. Chem.*, 2010, **55**(11), P. 1722–1739.
- [31] Fedorov P.P., Chernova E.V. Interactions of Yttrium and Lanthanum Fluorides with Other Fluorides. *J. Fluorine Chem.*, 2022, **263**, #110031 (9 pp.).
- [32] Fedorov P.P. *Investigation of phase diagrams of the CaF_2 –(Y,Ln) F_3 systems and polymorphism of rare earth trifluorides*. Thesis. M.: 1977. (in Russian)
- [33] Sobolev B.P. *The Rare Earth Trifluorides. P.2. Introduction to Materials Science of Multicomponent Metal Fluoride Crystals*. Barcelona, Institut d'Estudis Catalans, 2001.
- [34] Kuznetsov S.V., Fedorov P.P. Morphological Stability of Solid-Liquid Interface during Melt Crystallization of Solid Solutions $\text{M}_{1-x}\text{R}_x\text{F}_{2+x}$. *Inorg. Mater.*, 2008, **44**(13), P. 1434–1458. (Supplement).
- [35] Fedorov P.P. Association of point defects in non stoichiometric $\text{M}_{1-x}\text{R}_x\text{F}_{2+x}$ fluorite-type solid solutions. *Butll. Soc. Cat. Cien.*, 1991, **12**(2), P. 349–381.
- [36] Osiko V.V., Prokhorov A.M. *Investigation of the structure of crystals with an admixture of rare earth elements by spectroscopic methods. In: Problems of modern crystallography*. M.: Nauka, 1975, P. 280–301.
- [37] Cheetham A.K., Fender B.E.F., Steele D., Taylor R.I., Willis B.T.M. Defect structure of fluorite compounds containing excess anions. *Solid State Comm.*, 1970, **8**, P. 171–173.
- [38] Cheetham A.K., Fender B.E.F., Cooper M.J. Defect structure of calcium fluoride containing excess anions: Bragg scattering. *J. Phys. C: Solid State Phys.*, 1971, **4**, P. 3107–3121.
- [39] Allnatt A.R., Yuen P.S. Defect interactions in ionic fluorite structures: Pair clusters in CaF_2 doped by YF_3 . *J. Phys. C: Solid State Phys.*, 1975, **8**, P. 2199–2212.
- [40] Jacobs P.W.M., Ong S.H. Studies of defect clustering in $\text{CaF}_2:\text{Y}^{3+}$ by ionic conductivity and thermal depolarization. *J. Phys. Chem. Sol.*, 1980, **41**, P. 431–436.
- [41] Laval J.P., Frit B. Defect structure of anion-excess fluorite-related $\text{Ca}_{1-x}\text{Y}_x\text{F}_{2+x}$ solid solutions *J. Solid State Chem.*, 1983, **49**, P. 237–246.

- [42] Catlow C.R.A., Chadwick A.V., Corish J., Moroney L.M., O'Reilly A.N. Defect structure of doped CaF_2 at high temperatures. *Phys. Rev. B*, 1989, **39**(3), P. 1897–1906.
- [43] Hofmann M., Hull S., McIntyre G.J., Wilson C.C. A neutron diffraction study of the superionic transition in $(\text{Ca}_{1-x}\text{Y}_x)\text{F}_{2+x}$. *J. Phys.: Condens. Matter.*, 1997, **9**, P. 845–857.
- [44] Wang F., Grey C.P. Probing the defect structure of anion-excess $\text{Ca}_{1-x}\text{Y}_x\text{F}_{2+x}$ ($x = 0.03\text{--}0.32$) with high-resolution ^{19}F magic-angle spinning nuclear magnetic resonance spectroscopy. *Chem. Mater.*, 1998, **10**, P. 3081–3091.
- [45] Bevan D.J.M., Greis O., Strahle J. A new structural principle in anion-excess fluorite-related superlattices. *Acta Cryst.*, 1980, **36**(6), P. 889–890.
- [46] Bendall P.J., Catlow C.R.A., Corish J., Jacobs P.W.M. Defect aggregation in anion-excess fluorites. II. Clusters containing more than two impurity atoms. *J. Solid State Chem.*, 1984, **51**, P. 159–169.
- [47] Kazanskii S.A., Ryskin A.I., Nikiforov A.E., Zaharov A. Yu., Ougrumov M. Yu., Shakurov G.S. EPR spectra and crystal field of hexamer rare-earth clusters in fluorites. *Phys. Rev. B*, 2005, **72**, #014127 (11 pp).
- [48] Bagdasarov Kh. S., Voronko Yu.K., Kaminskii A.A., Krotova L.V., Osiko V.V. Modification of the optical properties of $\text{CaF}_2\text{--TR}^{3+}$ crystals by yttrium impurities. *Phys. stat. sol.*, 1965, **12**, P. 905–912.
- [49] Ivanov-Shits A.K., Sorokin N.I., Fedorov P.P., Sobolev B.P. Specific features of ionic transport in nonstoichiometric fluorite-type $\text{Ca}_{1-x}\text{R}_x\text{F}_{2+x}$ ($\text{R} = \text{La-Lu, Y, Sc}$) phases. *Solid State Ionics*, 1990, **37**, P. 125–137.
- [50] Sobolev B.P., Sorokin N.I., Bolotina N.B. Nonstoichiometric single crystals $\text{M}_{1-x}\text{R}_x\text{F}_{2+x}$ and $\text{R}_{1-y}\text{M}_y\text{F}_{3-y}$ ($\text{M} = \text{Ca, Sr, Ba, R}$ – rare earth elements) as fluorine-ionic conductive solid electrolytes. In: *Photonic and electronic properties of fluoride materials*. Ed. A. Tressaud, K. Poepelmeier. Amsterdam: Elsevier, 2016, P. 465–491.

Submitted 27 January 2023; revised 20 February 2023; accepted 27 March 2023

Information about the authors:

Alexander A. Alexandrov – Prokhorov General Physics Institute of the Russian Academy of Sciences, Vavilova str., 38, Moscow 119991, Russia; Kurnakov Institute of General and Inorganic Chemistry of the Russian Academy of Sciences, Leninskii pr. 31, Moscow, 119991, Russia; ORCID 0000-0001-7874-7284; alexandrov1996@yandex.ru

Anna D. Rezaeva – Prokhorov General Physics Institute of the Russian Academy of Sciences, Vavilova str., 38, Moscow 119991, Russia; ORCID 0000-0009-0005-9050-0184; 1032192969@rudn.ru

Vasilii A. Konyushkin – Prokhorov General Physics Institute of the Russian Academy of Sciences, Vavilova str., 38, Moscow 119991, Russia; ORCID 0000-0002-6028-8937; vasil@lst.gpi.ru

Andrey N. Nakladov – Prokhorov General Physics Institute of the Russian Academy of Sciences, Vavilova str., 38, Moscow 119991, Russia; ORCID 0000-0002-4060-8091; andy-nak@yandex.ru

Sergey V. Kuznetsov – Prokhorov General Physics Institute of the Russian Academy of Sciences, Vavilova str., 38, Moscow 119991, Russia; ORCID 0000-0002-7669-1106; kouznetzovsv@gmail.com

Pavel P. Fedorov – Prokhorov General Physics Institute of the Russian Academy of Sciences, Vavilova str., 38, Moscow 119991, Russia; ORCID 0000-0002-2918-3926; ppfedorov@yandex.ru

Conflict of interest: the authors declare no conflict of interest.